3D inversion of the time domain electromagnetic data for exploration of submarine hydrothermal deposits using the GEMTIP model

Masashi Endo, Leif Cox, and David Sunwall, TechnoImaging; Michael S. Zhdanov, TechnoImaging and The University of Utah; and Eiichi Asakawa, JGI*

Summary

This paper presents the results of an application of the time domain electromagnetic (TDEM) method for the exploration of submarine hydrothermal deposits using the generalized effective-medium relaxation model of the IP effect (GEMTIP). The TDEM data were acquired by a specially developed marine TDEM data acquisition system. It is known that the hydrothermal deposits consist of massive sulfides and can produce strong IP effect. In order to take this effect into account in interpretation of the observed data, we assume that the resistivity is frequency dependent and can be characterized by the GEMTIP relaxation model, including the chargeability, the time constant, and the relaxation parameter. The high chargeability anomaly determined by the 3D GEMTIP inversion coincides with the known submarine hydrothermal deposit. This opens a possibility to explore the submarine hydrothermal deposits effectively by marine TDEM method with 3D GEMTIP inversion.

Introduction

The Cabinet Office, Government of Japan (CAO) has established a project, Cross-ministerial Strategic Innovation Promotion Program (SIP), in order to develop an efficient next-generation technology for ocean resource exploration, as per the high potential of the submarine hydrothermal deposit and cobalt rich crust over huge offshore areas. J-MARES (Research and Development Partnership for Next Generation Technology of Marine Resources Survey) was organized to participate in the SIP. It aims to establish the multi-stage and integrated scheme for SMSs exploration by combining geophysical, geological and mineralogical exploration methods (Asakawa et al. 2016).

A comprehensive electromagnetic (EM) survey system, which includes EM data acquisition and interpretation of the EM data, has been developed as a part of this project. Since the target is more conductive than the host rocks, it is anticipated that EM method can be used as an effective exploration technique.

We have developed a prototype of the marine time-domain EM data acquisition system which can be towed by ROV and can acquire the dense EM data in relatively short time. A test survey was carried out over known hydrothermal deposit in Izena area, Japan, using the developed prototype of the marine time domain EM system.

In order to clarify the typical physical properties of the rocks forming the submarine hydrothermal deposit, we have conducted petrophysical and mineralogical analyses of the rock samples (Endo et al., 2016). The results of this analysis show that the target rocks (massive sulfides) produce strong induced polarization (IP) effect. This IP effect has to be taken into account in interpretation of observed EM data.

In the current paper, we invert the time domain electromagnetic data acquired over known submarine hydrothermal deposits in 3D with taking into account the IP effect by using the GEMTIP relaxation model.

Time domain electromagnetic survey over a submarine hydrothermal deposit

General geological setting and petrophysical analysis

The test EM survey was carried out in Izena area, Japan in 2015. There are several known hydrothermal deposits in the survey area. The typical deposit in this area forms mound with massive sulfides, and many chimneys and hydrothermal ejection holes are observed on/around the mound. Except for these mounds, the ocean bottom sediments cover the entire survey area. Therefore, an effective geophysical method is required to investigate the potential of non-typical offshore deposits.

We have studied the petrophysical and mineralogical characteristics of rock samples collected in the same survey area (Endo et al., 2016). Figure 1 shows an example of the result of QEMSCAN mineralogical analysis, and Table 1 shows result of the induced polarization (IP) analyses using GEMTIP relaxation model introduced by Zhdanov (2008). As expected, because of the large amount of sulfides, the rock samples from the hydrothermal deposit produce a strong IP effect. This fact indicates that the IP effect has to be taken into account in the interpretation of EM data acquired in the survey area.

Time domain electromagnetic survey

The time domain electromagnetic (TDEM) data were acquired in the survey area using the developed prototype of the marine TD EM data acquisition system. The system consists of transmitter-receiver loop (coincident loop configuration; 3.5 m x 3.5 m square loop with single turn), battery, and gyro-compass on one frame, and is towed by ROV with a speed of approximately 0.5 to 1 knot. Figure 2 shows a map of the survey lines with the sea-bottom bathymetry. As shown in this figure, there is a mound in the canter of the survey area, where the known submarine hydrothermal deposit exists.

Figure 3 presents an example of the TDEM data acquired along Line AA' as shown in Figure 2. As one can see, the EM signal in later time (later than 1 msec) is contaminated with high level of noise. Therefore, we used the TDEM data at earlier time only for the analysis and interpretation. One can see the anomalous field increasing in the area of mound in the profile (Figure 2b).

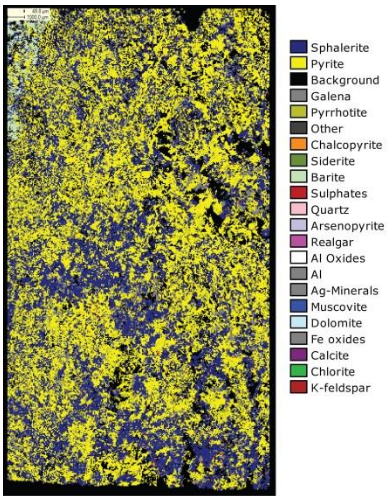

Mineral Name	%	area
Sphalerite	38.46	15767
Pyrite	35.77	14664
Background	9.16	3756
Galena	8.80	3608
Pyrrhotite	5.88	2412
Other	0.65	266
Chalcopyrite	0.43	175
Siderite	0.31	129
Barite	0.19	76
Sulphates	0.09	35
Quartz	0.08	32
Arsenopyrite	0.06	23
Realgar	0.05	21

Figure 1: Result of QEMSCAN mineralogical analysis.

Table 1: Result of GEMTIP analysis

	DC resistivity [Ohm-m]	Fraction volume [%]	Relaxation parameter [-]	Time constant [sec]
Matrix	50.4	-	-	-
Sphalerite	-	39.0	0.518	0.720
Pyrite	-	34.0	1.000	7.197

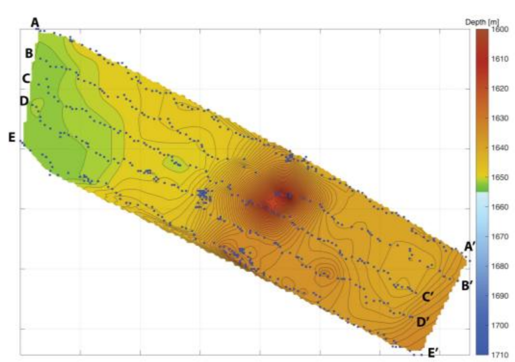

Figure 2: A map of the survey lines with the sea-bottom bathymetry.

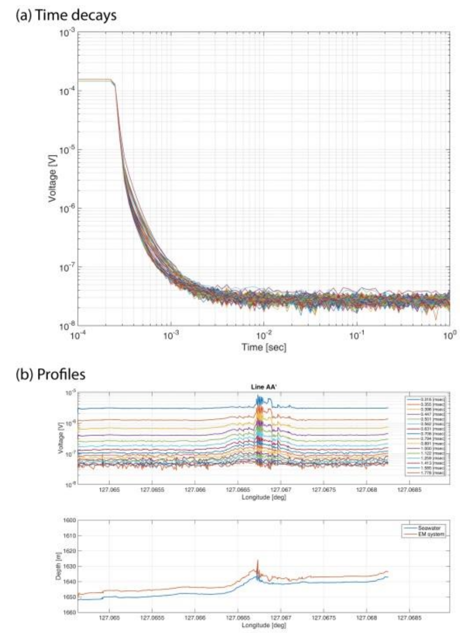

Figure 3: Plots of the measured EM (voltage) data at observation points along Line AA'; (a) time decays, (b) profiles.

3D inversion of marine time domain EM data

GEMTIP relaxation model

We inverted the observed time domain EM data using a two-phase GEMTIP relaxation model of the sea-bottom resistivity with taking into account the IP effect. The two-phase GEMTIP model with elliptical inclusions can be described by the following formula (Burtman et al., 2016);

$$\rho_e(\omega) = \rho_0 \left\{ 1 + \frac{f}{3} \sum_{\alpha = x,y,z} \frac{1}{\gamma_\alpha} \left[1 - \frac{1}{1 + s_\alpha (i\omega\tau)^C} \right] \right\}^{-1},$$

where ρ_0 is the DC resistivity (Ohm-m); f is the fraction volume; ω is the angular frequency (rad/sec); τ is the time constant; and C is the relaxation parameter. The coefficients γ_α and s_α $(\alpha = x, y, z)$ are the structural coefficients defined by the geometrical characteristics of the ellipsoidal inclusions used to approximate the grains:

$$s_\alpha = \frac{r_\alpha}{\bar{a}},$$

and $\bar{a}$ is an average value of the equatorial and polar radii of the ellipsoidal grains, and

$$r_\alpha = 2\frac{\gamma_\alpha}{\lambda_\alpha},$$

where γ_α and λ_α are the diagonal components of the volume surface depolarization tensors described in Burtman et al. (2016). The GEMTIP chargeability, η, can be expressed as follow:

$$\eta \approx \frac{3f}{1+3f}.$$

3D regularized inversion for the GEMTIP model parameters

We applied a 3D inversion method using a two-phase GEMTIP relaxation model of the sea-bottom structure to the observed time domain EM data.

The 3D inversion methodology consists of the 3D forward modeling based on the integral equation (IE) method and regularized 3D inversion based on the regularized conjugate gradient (RCG) method with adaptive regularization (Zhdanov, 2009, 2015).

The forward modeling of the TDEM data can be represented as following operator equation:

$$\mathbf{d} = A_G(\mathbf{m}),$$

where A_G is a GEMTIP forward modeling operator, and $\mathbf{m}$ is as vector of the GEMTIP model parameters $[\sigma, \eta, \tau, C]$.

The inversion is based on minimization of the Tikhonov parametric functional, $P^\alpha(\mathbf{m})$, with the corresponding stabilizing functional $S(\mathbf{m})$ (Zhdanov, 2002, 2015):

$$P^\alpha(\mathbf{m}) = \|\mathbf{W}_d(A_G(\mathbf{m}) - \mathbf{d})\|_{L_2}^2 + \alpha S(\mathbf{m}),$$

where $\mathbf{W}_d$ is the data-weighting matrix, and α is a regularization parameter. In the current project, we use the minimum norm stabilizer, S_{MN}, which is equal to the square L_2 norm of the difference between the current model $\mathbf{m}$ and an appropriate a priori model $\mathbf{m}_{apr}$:

$$S_{MN}(\mathbf{m}) = \left\|\mathbf{W}_m(\mathbf{m} - \mathbf{m}_{apr})\right\|_{L_2}^2,$$

where $\mathbf{W}_m$ is the weighting matrix of the model parameters.

The most common approach to minimization of the parametric functional $P^\alpha(\mathbf{m})$ is based on using gradient-type methods. We applied a regularized conjugate gradient (RCG) algorithm of the parametric functional minimization as described in Zhdanov (2002, 2015).

The appropriate selection of the data and the model parameters weighting matrices is very important for the success of the inversion. We determined the data weights as a diagonal matrix formed by the inverse absolute values of the background field (field of horizontally layered model). Computation of the model weighting matrix, $\mathbf{W}_m$, is based on sensitivity analysis. For the current study, we selected $\mathbf{W}_m$ as the square root of the sensitivity matrix for the model in each iteration:

$$\mathbf{W}_m^{(n)} = \sqrt{\mathrm{diag}\left(\mathbf{F}_{m_n}^* \mathbf{F}_{m_n}\right)}.$$

We applied the adaptive regularization method. The regularization parameter α was updated in the process of the iterative inversion as follows:

$$\alpha_n = \alpha_1 q^{n-1}; n = 1,2,3,\cdots; 0 < q < 1.$$

In order to avoid divergence, we begin an iteration from a value of α_1, which can be obtained as a ratio of the misfit and the stabilizing functionals for an initial model, then reduce α_n according to the last formula on each subsequent iteration and continuously iterate until the misfit condition reaches:

$$r_n^w = \|\mathbf{r}_n^w\| = \left\|\mathbf{W}_d\left(A_G\left(\mathbf{m}_{\alpha_n}\right) - \mathbf{d}\right)\right\| / \|\mathbf{W}_d \mathbf{d}\| \leq \delta,$$

where r_n^w is the normalized weighted residual, and δ is the relative level of noise in the weighted observed data.

The moving sensitivity domain approach was also applied to reduce the computational costs while keeping the accuracy of the computation.

The GEMTIP-based 3D inversion of the marine TDEM data

The developed algorithm was applied to the marine TDEM data collected in Izena area of Japan in 2015. The inversion parameters used for the 3D inversion are as follows:

- Inversion domain: 400 m x 150 m x 30 m
- Model discretization: 2 m x 2 m x 0.5 to 6 m (increasing logarithmically)
- Data: total 3,160

Figures 4 and 5 show 3D views of the conductivity and chargeability, respectively. One can clearly see that the conductive and chargeable anomalies appear in the area of a mound where the known submarine hydrothermal deposit exists.

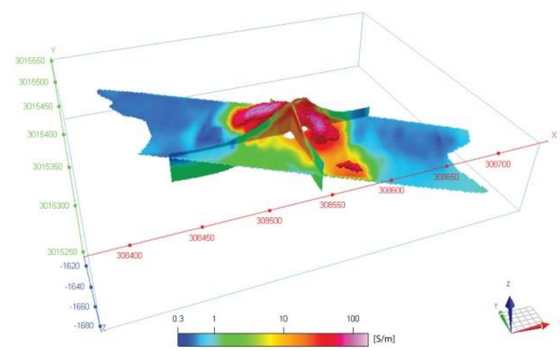

Figure 4: A 3D view of the 3D conductivity model recovered from the GEMTIP inversion of the marine time domain EM data.

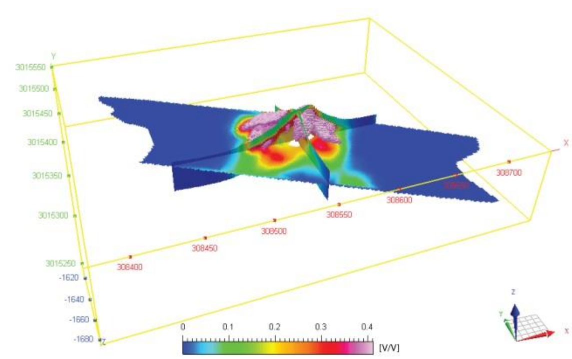

Figure 5: A 3D view of the 3D chargeability model recovered from the GEMTIP inversion of the marine time domain EM data.

Figures 6 through 8 show vertical cross-sections of 3D conductivity and chargeability models recovered from 3D GEMTIP inversion of time domain EM data along lines AA', BB', and CC'.

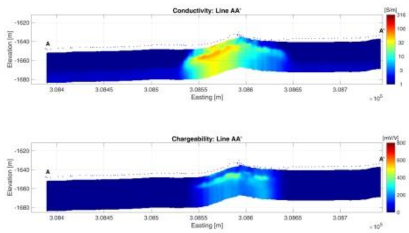

Figure 6: Vertical cross-sections of 3D conductivity (top) and chargeability (bottom) models along Line AA'.

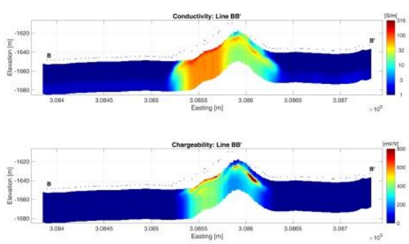

Figure 7: Vertical cross-sections of 3D conductivity (top) and chargeability (bottom) models along Line BB'.

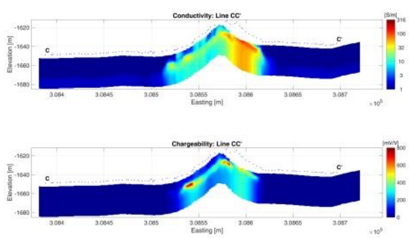

Figure 8: Vertical cross-sections of 3D conductivity (top) and chargeability (bottom) models along Line CC'.

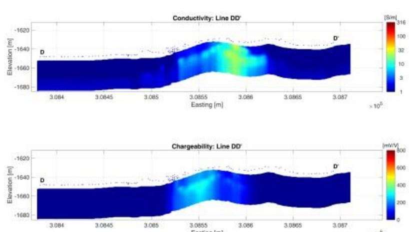

Figure 9: Vertical cross-sections of 3D conductivity (top) and chargeability (bottom) models along Line DD'.

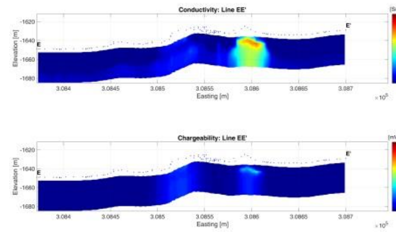

Figure 10: Vertical cross-sections of 3D conductivity (top) and chargeability (bottom) models along Line EE'.

Conclusions

We have presented the results of interpretation of the TDEM data acquired over a known submarine hydrothermal deposit by the developed marine TDEM data acquisition system. In our study, we took into account the strong IP effect, produced by the submarine hydrothermal deposit, using the GEMTIP relaxation model. The results of this study demonstrate that, even with limited EM data, we can locate a known submarine hydrothermal deposit as a high-conductivity and high-chargeability anomaly. This result opens a possibility for using the marine TDEM data for exploration of the submarine hydrothermal deposits.
Finally, we should note that, the developed GEMTIP inversion method can be applied to other marine CSEM (e.g., towed streamer EM) data as well, which, in general case, may contain information not only about the resistivity of the sea-bottom formations but also about the IP effect.

Acknowledgements

This work was supported by Council for Science, Technology and Innovation (CSTI), Cross-ministerial Strategic Innovation Promotion Program(SIP), "Next-generation technology for ocean resources exploration" (Lead agency: JAMSTEC). The authors acknowledge TechnoImaging, the University of Utah Consortium for Electromagnetic Modeling and Inversion (CEMI), and J-MARES for support of this project, and CAO and JAMSTEC for permission to publish. We also acknowledge Dr. Sangkyun Lee of JGI, Mr. Tomonori Sumi of NSENGI, Mr. Tadashi Yamakawa of MMTEC, and Dr. Akira Saito of Waseda University.

EDITED REFERENCES

Note: This reference list is a copyedited version of the reference list submitted by the author. Reference lists for the 2017 SEG Technical Program Expanded Abstracts have been copyedited so that references provided with the online metadata for each paper will achieve a high degree of linking to cited sources that appear on the Web.

REFERENCES

Asakawa, E., T. Sumi, T. Yamakawa, and M. Kose, 2016, Multi-stage and integrated approach for seafloor massive sulfide (SMS) exploration: Near Surface Geoscience — 1st Conference on Geophysics for Mineral Exploration and Mining, EAGE, Extended abstract, http://doi.org/10.3997/2214-4609.201602110.

Burtman, V., M. Endo, W. Lin, and M. S. Zhdanov, 2016, Complex resistivity of mineral rocks in the context of the generalized effective-medium theory of the IP effect: 86th Annual International Meeting, SEG, Expanded Abstracts, https://doi.org/10.1190/segam2016-13848294.1.

Endo, M., V. Burtman, E. U. Petersen, A. V. Gribenko, M. S. Zhdanov, S. Lee, and E. Asakawa, 2016, Induced polarization effect in rock samples collected from submarine hydrothermal deposit: Near Surface Geoscience — 1st Conference on Geophysics for Mineral Exploration and Mining, EAGE, Extended abstract, http://doi.org/10.3997/2214-4609.201602091.

Zhdanov, M. S., 2002, Geophysical inverse theory and regularization problems: Elsevier.

Zhdanov, M. S., 2008, Generalized effective-medium theory of induced polarization: Geophysics, **73**, no. 5, F197–F211, https://doi.org/10.1190/1.2973462.

Zhdanov, M. S., 2009, Geophysical electromagnetic theory and methods: Elsevier.

Zhdanov, M. S., 2015, Inverse theory and applications in geophysics: Elsevier.